

Research Article

Stability Analysis of Frictionless Planar Enveloping Grasps and Grasp Parameter Effects

Takayoshi Yamada¹, Hidehiko Yamamoto²¹Department of Mechanical Engineering, Gifu University, Yanagido 1-1, Gifu 501-1193, Japan²Gifu University, Yanagido 1-1, Gifu 501-1193, Japan

ARTICLE INFO

Article History

Received 26 November 2022

Accepted 06 September 2023

Keywords

Robot

Hand

Enveloping grasp

Grasp stability

Wrench vector

Grasp stiffness matrix

Curvature effect

Stiffness effect

ABSTRACT

This paper discusses quasi-static grasp stability of frictionless enveloping grasps in two dimensions. The stability is investigated from the viewpoint of potential energy stored in the grasps. The system of the grasps is replaced with elastic property, in which joint position and link surface properties are represented by linear stiffness. The contact constraints between a grasped object and finger links are formulated. The potential energy of the grasp system is obtained from the stiffness and the joint and link surface displacements. A wrench (i.e., force and moment) vector and a stiffness matrix of the grasp system are derived from partial differentiations by the pose (i.e., translation and rotation) displacement of the object. The grasps are stable if both the wrench vector is zero and the matrix is positive definite. The stability is evaluated by the eigenvalues of the matrix. Since, in this paper, the wrench vector and the stiffness matrix are derived in an analytical way, the matrix is given as a function of grasp positions, grasp forces, local curvatures, joint and surface stiffnesses, and so on at contact points, explicitly. We investigate curvature and stiffness effects on the grasp system by partially differentiating the matrix by the curvatures and stiffnesses. The positive definiteness of the matrix differentiations is analyzed. Validity of our analysis is confirmed through numerical examples.

© 2022 The Author. Published by Sugisaka Masanori at ALife Robotics Corporation Ltd.

This is an open access article distributed under the CC BY-NC 4.0 license

[\(http://creativecommons.org/licenses/by-nc/4.0/\)](http://creativecommons.org/licenses/by-nc/4.0/).

1. Introduction

Dexterous and flexible hands are inherent in human beings. The hands can grasp and manipulate objects of various shapes skillfully. In various fields like as production lines including assembly tasks, picking tasks, handling tasks, and so on, manual handworks by skillful workers are remained. Human hands are utilized for not only parts handling but also drilling and screw tightening with some tools. However, the handworks will be able to become bottlenecks in the production lines. Therefore, the human-like advanced technologies and methodologies are required for robots in mechanical functions.

Various types of grasp forms can be imagined like as pinching, enveloping, hooking, and so on. To avoid

squeezing, slipping out, breaking the parts, appropriate grasp forms (i.e., grasp types, grasp positions, grasp forces, etc.) are determined from the various types of grasps.

In order to obtain suitable grasps, machine learning methods are tackled in recent years. Siddiqui et al. [1], Li et al. [2], and Dong et al. [3] discussed grasp stability based on large amount of experimental data acquired from vision and/or force sensor. In general, the learning methods require strong CPU power, large amount of training data, and so on.

On the other hands, in traditional methodologies, grasp and manipulation of objects by multi-fingered hands are tackled from the viewpoint of mechanics, kinematics, statics, and dynamics in details. As one of the methods, Hanafusa et al. [4] and Nguyen [5] proposed a concept of

grasp stability. The stability was investigated from the viewpoint of potential energy stored in the grasp system. In the system, every finger displacement was replaced with linear elastic property. The stability expresses the index whether or not the grasp system returns to its initial pose (i.e., position and orientation) after external disturbance disappears. Watanabe [6] and Dong et al. [7] attacked effects of softness at contact points. In Ref. [8], we explored grasp stability of two spatial objects. Contact surface geometry (i.e., curvature, torsion, and metric tensor) was considered. Ref. [9] explored grasp stability of pinching grasps in which each finger is constructed of three revolute or prismatic joints. Effects of local curvatures on the stability were also tackled. Ref. [10] investigated grasp position effects on the grasp stability and proposed an algorithm for automatic generation of optimal grasp. In grasp forms, there are pinching grasps by fingertips, enveloping grasps by finger link surfaces, and so on. Refs. [4], [10] explored pinching grasps.

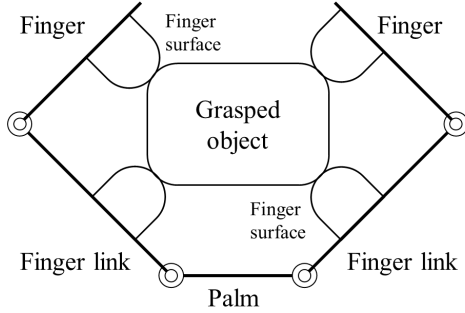


Figure 1: An enveloping grasp in two dimensions

In this paper, we explore quasi-static grasp stability of frictionless enveloping grasps in two dimensions (Figure 1). The grasp systems are analyzed by replacing joint position displacement and finger surface displacement with elastic model. In Section 2, displacement parameters, potential energies, and contact constraints are formulated. In Section 3, partial derivatives of the potential energy are derived. In Section 4, frictionless conditions at contact points are formulated and the wrench vector and stiffness matrix of the grasp system are derived. By using the eigenvalues of the matrix, the grasp stability is evaluated. In our formulation, the wrench and matrix are analytically derived, it is explicitly shown that the matrix is given as a function of grasp positions, grasp forces, local curvatures, joint and surface stiffnesses, and so on at contact points. In Section 5, we analyze curvature and

stiffness effects on the grasp system by partially differentiating the matrix by the curvatures and stiffnesses. In Section 6, we show a numerical example to confirm validity of our analysis. In Section 7, we show our conclusion.

2. Problem Formulation,

An object is enveloped by an m -fingered hand of which each finger consists of n -joints and links. We suppose that every link of the fingers is in contact with the object and the number of contact points of each link is one. Both every link and object surfaces are curved at the contact point but not overlapped each other.

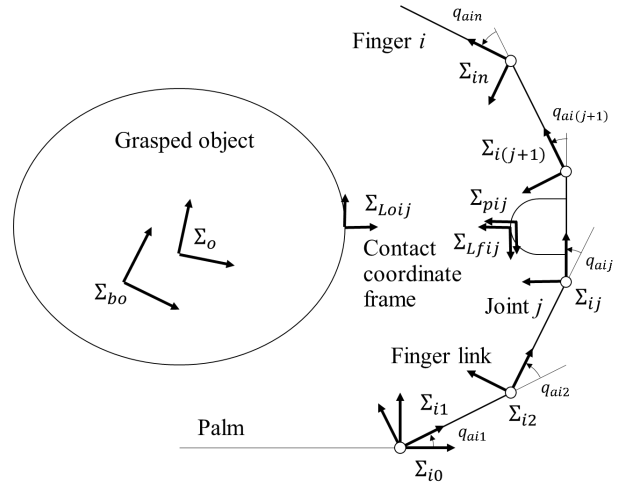


Figure 2: Object and finger coordinate frames

2.1. Notations

Finger number is denoted as i ($i = 1, 2, \dots, m$), and joint and link number is denoted as j ($j = 1, 2, \dots, n$). As shown in Figure 2, some coordinates are defined as follows:

- Σ_b : Base coordinate frame of the grasp system.
- Σ_o : Object coordinate frame fixed on the object.
- Σ_{bo} : Initial pose of Σ_o .
- Σ_{i0} : Base coordinate frame of the i -th finger.
- Σ_{ij} : Joint and link coordinate frame of the j -th joint of the i -th finger.
- Σ_{bij} : Initial pose of Σ_{ij} .
- $\Sigma_{coij}, \Sigma_{cfij}$: Contact coordinate frames on the object and finger surfaces, respectively.
- $\Sigma_{Loij}, \Sigma_{Lfij}$: Initial poses of Σ_{coij} and Σ_{cfij} , respectively.
- Σ_{pij} : Deformed coordinate frame of Σ_{Lfij} .

In Appendix A, we show vectors and matrices used in the following sections.

2.2. Displacements of joint position and finger surface

In this subsection, we explain position of each finger joint and pose of each finger link surface.

Configurations of the finger links are represented by positions of the finger joints. We define position of the j -th joint as symbol $q_{ajj} \in \mathbb{R}$, which is represented as the following components:

$$q_{ajj} = q_{naij} + q_{caij} + q_{daij}, \quad (j = 1, 2, \dots, n) \quad (1)$$

q_{naij}	Natural component
q_{caij}	Compressed component by the initial force
q_{daij}	Displaced component by the object displacement

The relative pose of Σ_{ij} with respect to $\Sigma_{i(j-1)}$ is represented as the following homogeneous transformation matrix:

$${}^{i(j-1)}A_{ij}(q_{ajj}) = \begin{cases} {}^{i(j-1)}A_{bij}(q_{naij}, q_{caij})A_r(q_{daij}) & \text{for revolute joint} \\ {}^{i(j-1)}A_{bij}(q_{naij}, q_{caij})A_t(q_{daij}\mathbf{u}_1) & \text{for prismatic joint} \end{cases} \quad (j = 1, 2, \dots, n) \quad (2)$$

The link surface is in contact on the object. We suppose that deformation of the link surface is approximated as the pose displacement of the surface coordinate. We define the deformation as symbol $\mathbf{q}_{pij} \in \mathbb{R}^3$, which is represented as the following components:

$$\mathbf{q}_{pij} = \mathbf{q}_{cpij} + \mathbf{q}_{dpij} \in \mathbb{R}^3, \quad (j = 1, 2, \dots, n) \quad (3)$$

\mathbf{q}_{cpij}	Compressed component by the initial force
\mathbf{q}_{dpij}	Displaced component by the object displacement

The relative pose of Σ_{Lfi} with respect to Σ_{ij} is represented by the following homogeneous transformation matrix:

$${}^{ij}A_{Lfi}(\mathbf{q}_{pij}) := {}^{ij}A_{pij}(\mathbf{q}_{cpij})A_{tr}(\mathbf{q}_{dpij}) \quad (4)$$

As a result, displacement parameters on the j -th link are summarized as the following vector:

$$\mathbf{q}_{dij} := [q_{daij}, \mathbf{q}_{dpij}^T]^T \in \mathbb{R}^4 \quad (5)$$

2.3. Potential energy of the grasp

We define an elastic coefficient of the joint position displacement as $s_{aij} \in \mathbb{R}$ and the potential energy of the j -th joint as

$$U_{aij}(q_{daij}) := \frac{1}{2} s_{aij} (q_{caij} + q_{daij})^2 \quad (6)$$

Initial joint torque $\tau_{aij} \in \mathbb{R}$ is formulated as

$$\tau_{aij} := s_{aij} q_{caij} \quad (7)$$

The coefficient s_{aij} is generated by some joint stiffness control and then is changeable. The torque τ_{aij} is also changeable by adjusting s_{aij} and q_{caij} .

We define a stiffness coefficient of the elasticity of the link surface displacement as $S_{pij} \in \mathbb{R}^{3 \times 3}$ and the potential energy of the j -th link of the i -th finger as

$$U_{pij}(\mathbf{q}_{dpij}) := \frac{1}{2} [\mathbf{q}_{cpij} + \mathbf{q}_{dpij}]^T S_{pij} [\mathbf{q}_{cpij} + \mathbf{q}_{dpij}] \quad (8)$$

Initial contact force $\boldsymbol{\tau}_{pij}$ is formulated as

$$\boldsymbol{\tau}_{pij} := S_{pij} \mathbf{q}_{cpij} \quad (9)$$

The coefficient matrix S_{pij} is inherent in the mechanical surface property.

We obtain the potential energy of the i -th finger as

$$U_i(\mathbf{q}_{di}) := \sum_{j=1}^n \{U_{aij}(q_{daij}) + U_{pij}(\mathbf{q}_{dpij})\} \quad (10)$$

where the symbol \mathbf{q}_{di} is defined as the following vector.

$$\mathbf{q}_{di} := [q_{di1}^T, \dots, q_{din}^T]^T \in \mathbb{R}^{4n} \quad (11)$$

Since the number of fingers is denoted as m , we obtain the potential energy of the grasp system as

$$U(\mathbf{q}_d) := \sum_{i=1}^m U_i(\mathbf{q}_{di}), \quad \mathbf{q}_d := [q_{d1}^T, \dots, q_{dm}^T]^T \quad (12)$$

2.4. Contact constraints of the object and finger link surfaces

Since the j -th link surface is in contact on the object, the contact constraint is given by the following formula.

$$\begin{aligned} & {}^b A_{bo} {}^{bo} A_o(\boldsymbol{\varepsilon}_o) {}^o A_{Loij} {}^{Loij} A_{Coi}(\alpha_{oij}) \\ &= {}^b A_{i0} {}^{i0} A_{i1}(q_{ai1}) \times \dots \times {}^{i(j-1)} A_{ij}(q_{ajj}) \\ & \times {}^{ij} A_{Lfi}(\mathbf{q}_{pij}) {}^{Lfi} A_{Cfi}(\alpha_{fij}) {}^{Cfi} A_{Coi} \end{aligned} \quad (j = 1, 2, \dots, n) \quad (13)$$

The parameter $\boldsymbol{\varepsilon}_o \in \mathbb{R}^3$ denotes pose (i.e., position and orientation) displacement of the object. The parameters $\alpha_{oij} \in \mathbb{R}$ and $\alpha_{fij} \in \mathbb{R}$ denote the contact point displacements on the object and link surfaces, respectively.

$$\begin{aligned} {}^{Loij} A_{Coi}(\alpha_{oij}) &:= {}^{Loij} A_{\kappa oij} A_r(\kappa_{oij} \alpha_{oij}) {}^{Loij} A_{\kappa oij}^{-1} \\ {}^{Lfi} A_{Cfi}(\alpha_{fij}) &:= {}^{Lfi} A_{\kappa fij} A_r(\kappa_{fij} \alpha_{fij}) {}^{Lfi} A_{\kappa fij}^{-1} \end{aligned} \quad (14)$$

where the matrices ${}^{Loij} A_{\kappa oij}$ and ${}^{Lfi} A_{\kappa fij}$ are defined as the following forms:

$${}^{Loij} A_{\kappa oij} := A_t(-\kappa_{oij}^{-1} \mathbf{u}_1), \quad {}^{Lfi} A_{\kappa fij} := A_t(-\kappa_{fij}^{-1} \mathbf{u}_1) \quad (15)$$

Local curvature at contact point is denoted as κ . If the curvature κ is positive, zero, or negative, then the surface is convex, flat, or concave, respectively. Because of no overlapping between the object and finger link surfaces, we have $\kappa_{oij} + \kappa_{fij} > 0$. Since the link surface contacts

on the object surface, the relation between Σ_{Cfij} and Σ_{Coij} is given as

$${}^{cfij}A_{Coij} = A_r(\pi) \quad (16)$$

From the contact constraint (13), we obtain

$$\begin{aligned} A_{tr}(\mathbf{q}_{dpij}) &= {}^{pij}A_{ij} {}^{i(j-1)}A_{ij}^{-1}(\mathbf{q}_{aij}) \times \dots \\ &\times {}^{i0}A_{i1}^{-1}(\mathbf{q}_{ai1}) {}^{i0}A_{bo} {}^{bo}A_o(\boldsymbol{\varepsilon}_o) {}^oA_{Loij} \\ &\times {}^{Loij}A_{Coij}(\boldsymbol{\alpha}_{oij}) {}^{cfij}A_{Coij}^{-1} {}^{Lfij}A_{Cfij}^{-1}(\boldsymbol{\alpha}_{fij}) \end{aligned} \quad (17)$$

The surface displacement \mathbf{q}_{dpij} depends on the object displacement $\boldsymbol{\varepsilon}_o$, joint position displacement q_{daij} ($k = 1, 2, \dots, j$), and contact position displacement $\boldsymbol{\alpha}_{ij}$.

$$\mathbf{q}_{dpij}(\boldsymbol{\varepsilon}_o, \boldsymbol{\alpha}_{ij}, q_{dai1}, \dots, q_{daij}), \quad (j = 1, 2, \dots, n) \quad (18)$$

where the symbol $\boldsymbol{\alpha}_{ij}$ is defined as the following vector.

$$\boldsymbol{\alpha}_{ij} := \begin{bmatrix} \alpha_{oij} \\ \alpha_{fij} \end{bmatrix} \in \mathbb{R}^2 \quad (19)$$

Consequently, the energy (10) is transformed to

$$\begin{aligned} U_{iq}(\boldsymbol{\varepsilon}_o, \boldsymbol{\alpha}_i, \boldsymbol{\beta}_i) &:= \\ &= \sum_{j=1}^n \left\{ U_{aij}(q_{daij}) \right. \\ &\left. + U_{pij}(\mathbf{q}_{dpij}(\boldsymbol{\varepsilon}_o, \boldsymbol{\alpha}_{ij}, q_{dai1}, \dots, q_{daij})) \right\} \end{aligned} \quad (20)$$

where the symbols $\boldsymbol{\alpha}_i$ and $\boldsymbol{\beta}_i$ are defined as the following vectors:

$$\boldsymbol{\alpha}_i := \begin{bmatrix} \alpha_{i1} \\ \vdots \\ \alpha_{in} \end{bmatrix} \in \mathbb{R}^{2n}, \quad \boldsymbol{\beta}_i := \begin{bmatrix} q_{dai1} \\ \vdots \\ q_{dain} \end{bmatrix} \in \mathbb{R}^n \quad (21)$$

3. Partial derivatives of the potential energy

3.1. The first partial derivatives

In this subsection, we show the first partial derivatives of the potential energy by $\boldsymbol{\varepsilon}_o$, $\boldsymbol{\alpha}_i$, and $\boldsymbol{\beta}_i$. Considering the initial condition, we have the following vectors:

$$\begin{aligned} U_{iq,\varepsilon} &:= \frac{\partial U_{iq}(\boldsymbol{\varepsilon}_o, \boldsymbol{\alpha}_i, \boldsymbol{\beta}_i)}{\partial \boldsymbol{\varepsilon}_o} \Big|_0 = \sum_{j=1}^n {}^{Lfij}B_o^T \boldsymbol{\tau}_{pij} \in \mathbb{R}^3 \\ U_{iq,\alpha} &:= \frac{\partial U_{iq}(\boldsymbol{\varepsilon}_o, \boldsymbol{\alpha}_i, \boldsymbol{\beta}_i)}{\partial \boldsymbol{\alpha}_i} \Big|_0 = \begin{bmatrix} U_{iq,\alpha_1} \\ \vdots \\ U_{iq,\alpha_n} \end{bmatrix} \in \mathbb{R}^{2n} \\ U_{iq,\beta} &:= \frac{\partial U_{iq}(\boldsymbol{\varepsilon}_o, \boldsymbol{\alpha}_i, \boldsymbol{\beta}_i)}{\partial \boldsymbol{\beta}_i} \Big|_0 = \begin{bmatrix} U_{iq,q_1} \\ \vdots \\ U_{iq,q_n} \end{bmatrix} \in \mathbb{R}^n \end{aligned} \quad (22)$$

where the elements U_{iq,α_k} and U_{iq,q_k} are obtained as

$$\begin{aligned} U_{iq,\alpha_k} &:= \frac{\partial U_{iq}(\boldsymbol{\varepsilon}_o, \boldsymbol{\alpha}_i, \boldsymbol{\beta}_i)}{\partial \alpha_{ik}} \Big|_0 = K_{ik}^T \boldsymbol{\tau}_{pik} \in \mathbb{R}^2 \\ K_{ik} &:= \begin{bmatrix} -\mathbf{u}_2 & -\mathbf{u}_2 \\ \kappa_{oik} & -\kappa_{fik} \end{bmatrix} \in \mathbb{R}^{3 \times 2} \end{aligned}$$

$$\begin{aligned} U_{iq,q_k} &:= \frac{\partial U_{iq}(\boldsymbol{\varepsilon}_o, \boldsymbol{\alpha}_i, \boldsymbol{\beta}_i)}{\partial q_{daij}} \Big|_0 \\ &= \tau_{aik} - \mathbf{v}_\zeta^T \sum_{j=k}^n {}^{Lfij}B_{ik}^T \boldsymbol{\tau}_{pij} \in \mathbb{R} \end{aligned} \quad (23)$$

The detailed derivations are omitted for page space.

3.2. The second partial derivatives

In this subsection, we show the second partial derivatives of the potential energy by $\boldsymbol{\varepsilon}_o$, $\boldsymbol{\alpha}_i$, and $\boldsymbol{\beta}_i$. Considering the initial condition, we have the following matrices:

$$\begin{aligned} U_{iq,\varepsilon\varepsilon} &:= \frac{\partial^2 U_{iq}(\boldsymbol{\varepsilon}_o, \boldsymbol{\alpha}_i, \boldsymbol{\beta}_i)}{\partial \boldsymbol{\varepsilon}_o \partial \boldsymbol{\varepsilon}_o^T} \Big|_0 \\ &= \sum_{j=1}^n \left\{ {}^{Lfij}B_o^T S_{pij} {}^{Lfij}B_o + \mathbf{v}_\zeta ({}^{Lfij} \mathbf{p}_o^T I_{23} \boldsymbol{\tau}_{pij}) \mathbf{v}_\zeta^T \right\} \\ &\in \mathbb{R}^{3 \times 3} \\ U_{iq,\alpha\varepsilon}^T &= U_{iq,\varepsilon\alpha} := \frac{\partial^2 U_{iq}(\boldsymbol{\varepsilon}_o, \boldsymbol{\alpha}_i, \boldsymbol{\beta}_i)}{\partial \boldsymbol{\varepsilon}_o \partial \boldsymbol{\alpha}_i^T} \Big|_0 \\ &= [U_{iq,\varepsilon\alpha_1} \ \dots \ U_{iq,\varepsilon\alpha_n}] \in \mathbb{R}^{3 \times 2n} \\ U_{iq,\beta\varepsilon}^T &= U_{iq,\varepsilon\beta} := \frac{\partial^2 U_{iq}(\boldsymbol{\varepsilon}_o, \boldsymbol{\alpha}_i, \boldsymbol{\beta}_i)}{\partial \boldsymbol{\varepsilon}_o \partial \boldsymbol{\beta}_i^T} \Big|_0 \\ &= [U_{iq,\varepsilon q_1} \ \dots \ U_{iq,\varepsilon q_n}] \in \mathbb{R}^{3 \times n} \\ U_{iq,\alpha\alpha} &:= \frac{\partial^2 U_{iq}(\boldsymbol{\varepsilon}_o, \boldsymbol{\alpha}_i, \boldsymbol{\beta}_i)}{\partial \boldsymbol{\alpha}_i \partial \boldsymbol{\alpha}_i^T} \Big|_0 \\ &= \begin{bmatrix} U_{iq,\alpha_1\alpha_1} & \dots & U_{iq,\alpha_1\alpha_n} \\ \vdots & \ddots & \vdots \\ U_{iq,\alpha_n\alpha_1} & \dots & U_{iq,\alpha_n\alpha_n} \end{bmatrix} \in \mathbb{R}^{2n \times 2n} \\ U_{iq,\alpha\beta}^T &= U_{iq,\beta\alpha} := \frac{\partial^2 U_{iq}(\boldsymbol{\varepsilon}_o, \boldsymbol{\alpha}_i, \boldsymbol{\beta}_i)}{\partial \boldsymbol{\beta}_i \partial \boldsymbol{\alpha}_i^T} \Big|_0 \\ &= \begin{bmatrix} U_{iq,q_1\alpha_1} & \dots & U_{iq,q_1\alpha_n} \\ \vdots & \ddots & \vdots \\ U_{iq,q_n\alpha_1} & \dots & U_{iq,q_n\alpha_n} \end{bmatrix} \in \mathbb{R}^{n \times 2n} \\ U_{iq,\beta\beta} &:= \frac{\partial^2 U_{iq}(\boldsymbol{\varepsilon}_o, \boldsymbol{\alpha}_i, \boldsymbol{\beta}_i)}{\partial \boldsymbol{\beta}_i \partial \boldsymbol{\beta}_i^T} \Big|_0 \\ &= \begin{bmatrix} U_{iq,q_1q_1} & \dots & U_{iq,q_1q_n} \\ \vdots & \ddots & \vdots \\ U_{iq,q_nq_1} & \dots & U_{iq,q_nq_n} \end{bmatrix} \in \mathbb{R}^{n \times n} \end{aligned} \quad (24)$$

The details of the elements are shown in Appendix B.

4. Enveloping grasps with frictionless sliding contact

4.1. Frictionless constraints at contacts

Since the finger link surface is in contact on the object with frictionless sliding, the contact point displacement $\boldsymbol{\alpha}_i$ and the joint position displacement $\boldsymbol{\beta}_i$ have to locally

minimize the energy. Consequently, the following constraints are handled:

$$\frac{\partial U_{iq}(\boldsymbol{\varepsilon}_o, \boldsymbol{\alpha}_i, \boldsymbol{\beta}_i)}{\partial \boldsymbol{\alpha}_i} = \mathbf{0}_{2n} \quad (25.1)$$

$$\frac{\partial U_{iq}(\boldsymbol{\varepsilon}_o, \boldsymbol{\alpha}_i, \boldsymbol{\beta}_i)}{\partial \boldsymbol{\beta}_i} = \mathbf{0}_n \quad (25.2)$$

From (25.1) at the initial condition, we have $U_{iq, \alpha_k} = 0_2$. Using (23), we have the following contact force:

$$\boldsymbol{\tau}_{pik} = I_{23}^T L^{fik} \mathbf{f}, \quad L^{fik} \mathbf{f} = \begin{bmatrix} L^{fik} f_x \\ L^{fik} f_y \end{bmatrix} \in \mathbb{R}^2, \quad (26)$$

$$L^{fik} f_x < 0, \quad L^{fik} f_y = 0$$

The symbol $L^{fik} f_x$ and $L^{fik} f_y$ are normal and tangential components of the contact force, respectively. Because the contact force $L^{fik} \mathbf{f}$ is represented in the frame $\Sigma_{L^{fik}}$, $L^{fik} f_x$ is negative. From (25.2) at the initial condition, we have $U_{iq, q_k} = 0$. Using (23), we have the following joint torque:

$$\boldsymbol{\tau}_{aik} = \mathbf{v}_\zeta^T \sum_{j=k}^n L^{fij} \mathbf{B}_{ik}^T \boldsymbol{\tau}_{pij} \quad (27)$$

Since (25) has $3n$ constraints, the number of independent parameters of the grasp system is reduced to three. Finally, the displacements $\boldsymbol{\alpha}_i$ and $\boldsymbol{\beta}_i$ are given by functions of the parameter $\boldsymbol{\varepsilon}_o$.

$$U_{iq}^{fs}(\boldsymbol{\varepsilon}_o) := U_{iq}(\boldsymbol{\varepsilon}_o, \boldsymbol{\alpha}_i(\boldsymbol{\varepsilon}_o), \boldsymbol{\beta}_i(\boldsymbol{\varepsilon}_o)) \quad (28)$$

Considering (25), the following gradient is obtained.

$$G_i^{fs} := \left. \frac{\partial U_{iq}^{fs}(\boldsymbol{\varepsilon}_o)}{\partial \boldsymbol{\varepsilon}_o} \right|_0 = \sum_{j=1}^n {}^o W_{L^{fij}} L^{fij} \mathbf{f} \quad (29)$$

Deriving partial derivative of (25) by the object displacement $\boldsymbol{\varepsilon}_o$, we have the following formula:

$$Q_i^{fs} := \left[\left. \frac{\partial \boldsymbol{\alpha}_i^T}{\partial \boldsymbol{\varepsilon}_o} \right|_0 \quad \left. \frac{\partial \boldsymbol{\beta}_i^T}{\partial \boldsymbol{\varepsilon}_o} \right|_0 \right] \\ = -[U_{iq, \varepsilon \alpha} \quad U_{iq, \varepsilon \beta}] \begin{bmatrix} U_{iq, \alpha \alpha} & U_{iq, \alpha \beta} \\ U_{iq, \beta \alpha} & U_{iq, \beta \beta} \end{bmatrix}^{-1} \in \mathbb{R}^{3 \times 3n} \quad (30)$$

The second partial derivative of $U_{iq}^{fs}(\boldsymbol{\varepsilon}_o)$ is obtained as

$$H_i^{fs} := \left. \frac{\partial^2 U_{iq}^{fs}(\boldsymbol{\varepsilon}_o)}{\partial \boldsymbol{\varepsilon}_o \partial \boldsymbol{\varepsilon}_o^T} \right|_0 = U_{iq, \varepsilon \varepsilon} + Q_i^{fs} \begin{bmatrix} U_{iq, \alpha \varepsilon} \\ U_{iq, \beta \varepsilon} \end{bmatrix} \quad (31)$$

We have the potential energy of the grasp system as

$$U^{fs}(\boldsymbol{\varepsilon}_o) := \sum_{i=1}^m U_{iq}^{fs}(\boldsymbol{\varepsilon}_o) \quad (32)$$

Total grasp wrench G^{fs} and grasp stiffness matrix H^{fs} are given by

$$G^{fs} := \left. \frac{\partial U^{fs}(\boldsymbol{\varepsilon}_o)}{\partial \boldsymbol{\varepsilon}_o} \right|_0 = \sum_{i=1}^m G_i^{fs} \in \mathbb{R}^3 \\ H^{fs} := \left. \frac{\partial^2 U^{fs}(\boldsymbol{\varepsilon}_o)}{\partial \boldsymbol{\varepsilon}_o \partial \boldsymbol{\varepsilon}_o^T} \right|_0 = \sum_{i=1}^m H_i^{fs} \in \mathbb{R}^{3 \times 3} \quad (33)$$

If $G^{fs} = \mathbf{0}_3$ and $H^{fs} > \mathbf{0}_{3 \times 3}$ at the initial condition, then the grasp is stable. The condition $G^{fs} = \mathbf{0}$ means that the grasp is in wrench equilibrium. The condition $H^{fs} > \mathbf{0}_{3 \times 3}$ means that the matrix is positive definite, and the grasp returns to the initial pose after external disturbances disappear. Using the eigenvalues and eigenvectors of the matrix H^{fs} , we can evaluate the grasp stability.

5. Effect of grasp parameters

The matrix H^{fs} depends on grasp parameters which include contact positions, contact directions, contact forces, local curvatures, stiffness properties at the contact points. In our formulation, the matrix is analytically derived. We can differentiate the matrix by the grasp parameters.

5.1. Partial derivative of the local curvatures

In this subsection, we derive effects of the local curvatures at contact points. Partially differentiation of the stiffness matrix H_i^{fs} by the local curvature κ_{oij} yields the following matrix:

$$\frac{\partial H_i^{fs}}{\partial \kappa_{oij}} = \frac{\partial U_{iq, \varepsilon \varepsilon}}{\partial \kappa_{oij}} + \left\{ \frac{\partial}{\partial \kappa_{oij}} \begin{bmatrix} U_{iq, \varepsilon \alpha} \\ U_{iq, \varepsilon \beta} \end{bmatrix} \right\}^T [Q_i^{fs}]^T \\ + Q_i^{fs} \left\{ \frac{\partial}{\partial \kappa_{oij}} \begin{bmatrix} U_{iq, \varepsilon \alpha} \\ U_{iq, \varepsilon \beta} \end{bmatrix} \right\} \\ + Q_i^{fs} \left\{ \frac{\partial}{\partial \kappa_{oij}} \begin{bmatrix} U_{iq, \alpha \alpha} & U_{iq, \alpha \beta} \\ U_{iq, \beta \alpha} & U_{iq, \beta \beta} \end{bmatrix} \right\} [Q_i^{fs}]^T \\ = L^{fij} f_x \mathbf{b}_{oij} \mathbf{b}_{oij}^T \preceq \mathbf{0}_{3 \times 3} \quad (34)$$

The derivatives $\frac{\partial U_{iq, \varepsilon \varepsilon}}{\partial \kappa_{oij}}$, $\frac{\partial U_{iq, \varepsilon \alpha}}{\partial \kappa_{oij}}$, ... are briefly shown in Appendix C. In a similar manner, we have the following matrix:

$$\frac{\partial H_i^{fs}}{\partial \kappa_{fij}} = L^{fij} f_x \mathbf{b}_{fij} \mathbf{b}_{fij}^T \preceq \mathbf{0}_{3 \times 3} \quad (35)$$

where the vectors \mathbf{b}_{oij} and $\mathbf{b}_{fij} \in \mathbb{R}^3$ are given by

$$\mathbf{b}_{oij} := Q_i^{fs} \begin{bmatrix} \mathbf{0}_{2(j-1) \times 1} \\ \mathbf{u}_1 \\ \mathbf{0}_{2(n-j) \times 1} \\ \mathbf{0}_{n \times 1} \end{bmatrix}, \quad \mathbf{b}_{fij} := Q_i^{fs} \begin{bmatrix} \mathbf{0}_{2(j-1) \times 1} \\ \mathbf{u}_2 \\ \mathbf{0}_{2(n-j) \times 1} \\ \mathbf{0}_{n \times 1} \end{bmatrix} \quad (36)$$

Because we have $L^{fij} f_x < 0$, the derivatives $\partial H_i^{fs} / \partial \kappa_{oij}$ and $\partial H_i^{fs} / \partial \kappa_{fij}$ are negative semi-definite. It is shown that the values of the local curvatures are made small, the grasp stability is enhanced. Its directions are given by the vectors \mathbf{b}_{oij} and \mathbf{b}_{fij} , respectively.

5.2. Partial derivative of the spring stiffnesses

In this subsection, we derive effects of the spring stiffnesses. Partially differentiation of the matrix H_i^{fs} by the joint stiffness s_{aij} yields the following formula:

$$\frac{\partial H_i^{fs}}{\partial s_{aij}} = \mathbf{b}_{saij} \mathbf{b}_{saij}^T \geq \mathbf{0}_{3 \times 3} \quad (37)$$

$$\mathbf{b}_{saij} := Q_i^{fs} \begin{bmatrix} 0_{2n \times 1} \\ 0_{(j-1) \times 1} \\ 1 \\ 0_{(n-j) \times 1} \end{bmatrix} \in \mathbb{R}^3$$

In the case that the surface stiffness is given by $S_{pij} = \text{diag}[s_{pijx}, s_{pijy}, s_{pijz}]$, the partial derivatives of H_i^{fs} by these elements are obtained by

$$\begin{aligned} \frac{\partial H_i^{fs}}{\partial s_{pijx}} &= \mathbf{b}_{spijx} \mathbf{b}_{spijx}^T \geq \mathbf{0}_{3 \times 3} \\ \frac{\partial H_i^{fs}}{\partial s_{pijy}} &= \mathbf{b}_{spijy} \mathbf{b}_{spijy}^T \geq \mathbf{0}_{3 \times 3} \\ \frac{\partial H_i^{fs}}{\partial s_{pijz}} &= \mathbf{b}_{spijz} \mathbf{b}_{spijz}^T \geq \mathbf{0}_{3 \times 3} \end{aligned} \quad (38)$$

where the vectors $\mathbf{b}_{spijx}, \mathbf{b}_{spijy}, \mathbf{b}_{spijz} \in \mathbb{R}^3$ and the matrix $C_{ij} \in \mathbb{R}^{3 \times 3}$ are given by

$$\begin{aligned} \mathbf{b}_{spijx} &:= C_{ij} \mathbf{v}_x, \quad \mathbf{b}_{spijy} := C_{ij} \mathbf{v}_y, \\ \mathbf{b}_{spijz} &:= C_{ij} \mathbf{v}_z \\ C_{ij} &:= \left\{ \begin{array}{l} L^{fij} B_o^T + Q_i^{fs} \\ \left[\begin{array}{l} 0_{2(j-1) \times 3} \\ K_{ij}^T \\ 0_{2(n-j) \times 3} \\ \mathbf{v}_z^T L^{fij} B_{i1}^T \\ \vdots \\ \mathbf{v}_z^T L^{fij} B_{ij}^T \\ 0_{(n-j) \times 3} \end{array} \right] \end{array} \right\} \end{aligned} \quad (39)$$

The derivatives $\frac{\partial H_i^{fs}}{\partial s_{aij}}, \frac{\partial H_i^{fs}}{\partial s_{pijx}}, \frac{\partial H_i^{fs}}{\partial s_{pijy}}$, and $\frac{\partial H_i^{fs}}{\partial s_{pijz}}$ are positive semi-definite. It is shown that the parameter $s_{aij}, s_{pijx}, s_{pijy}$ and s_{pijz} are larger, positive definiteness of the stiffness matrix are larger. Its corresponding directions are also obtained as $\mathbf{b}_{saij}, \mathbf{b}_{spijx}, \mathbf{b}_{spijy}$ and \mathbf{b}_{spijz} .

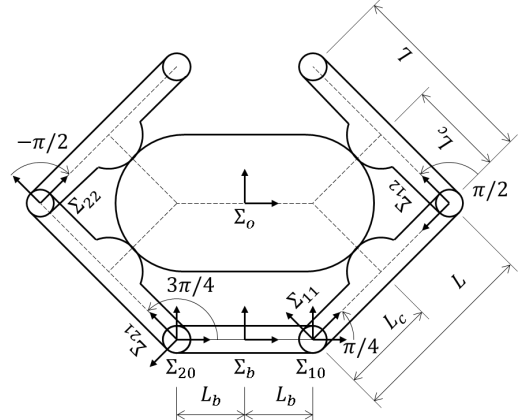
6. Numerical examples

As shown in (2), in this paper, we treated not only revolute but also prismatic joint type. Due to page space, in this section, we only consider the revolute type.

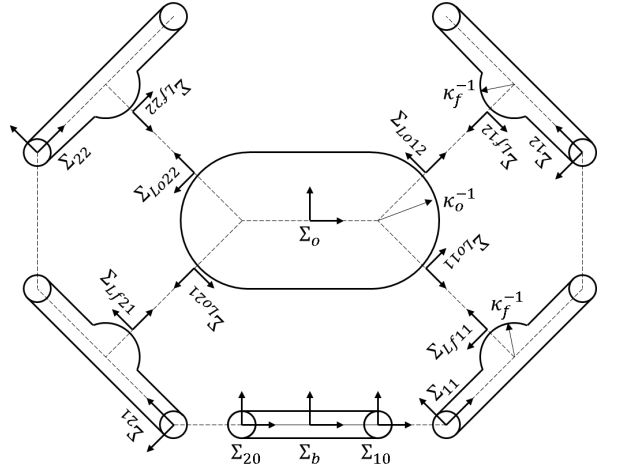
As shown in Figure 3, we investigate the grasp that an object enveloped by a 2-finger 4-joint hand. In this example, the grasp is symmetric. The link lengths, local curvatures, and spring stiffnesses are set as follows:

$$\begin{aligned} L_b &= 0.010 \text{ m}, L = 0.030 \text{ m}, L_c = 0.015 \text{ m}, \\ \kappa_o &= 100 \text{ m}^{-1}, \kappa_f = 200 \text{ m}^{-1}, s_{aij} = 10 \text{ Nm/rad}, \\ S_{pij} &= \text{diag}[500 \text{ N/m} \quad 500 \text{ N/m} \quad 10 \text{ Nm/rad}] \end{aligned} \quad (40)$$

For simplicity of discussion, the lengths of all finger links are same, the contact positions on the links are intermediate on the links, and the surface curvatures are convex. The center of the local curvature at contact point on each link surface are located on the link axis. The centers of the local curvatures at contact points on the object with the i -th finger are located at one point.



(a) Link coordinate frames, link lengths, and joint angles



(b) Contact coordinate frames and local curvatures

Figure 3: Numerical example of an enveloping grasp

In this example, the grasp will be stable. We show the grasp stiffness matrix, and eigenvalues and eigenvectors of the matrix. Moreover, we show the directions of the curvature and stiffness effects.

The grasp stiffness matrix is calculated as

$$H^{fs} = \begin{bmatrix} 620.7 & 0 & -0.092 \\ 0 & 630.1 & 0 \\ -0.092 & 0 & 0.01 \end{bmatrix} \quad (41)$$

As shown in (41), not only diagonal elements but also interference elements between x-translation and rotation appear. The eigenvalues and eigenvectors of H^{fs} are shown in Table 1. In this grasp, all eigenvalues are positive, then the grasp is stable. In the first mode, the object displacement is obtained in y translation. In the second mode, the object displacement is mainly obtained in x translation. In the third mode, the object displacement is mainly obtained in rotation.

Table 2 shows the direction vectors of the parameter effects. The vectors \mathbf{b}_{o11} , \mathbf{b}_{f11} , \mathbf{b}_{o12} , and \mathbf{b}_{f12} express curvature effects, then these appear in tangential directions at contact points. The vectors \mathbf{b}_{sp11x} , \mathbf{b}_{sp11y} , \mathbf{b}_{sp12x} , \mathbf{b}_{sp12y} express stiffness effects at the corresponding contact points, then these appear in vertical direction at contact surface.

Table 1: Eigenvalues and eigenvectors of the grasp

mode p	Eigenvalues $\lambda_p(H^{fs})$	Eigenvectors $\mathbf{v}_p(H^{fs})$
1	630.1	$[0, 1, 0]^T$
2	620.7	$[1.00, 0, 0.00]^T$
3	0.0064	$[0.00, 0, 1.00]^T$

Table 2: Direction vectors of the parameter effects for $i = 1$. (The case of $i = 2$ is omitted for page space.)

j	κ_{oij}	κ_{fij}	s_{aij}
1	\mathbf{b}_{o11} $= \begin{bmatrix} -0.64 \\ -0.64 \\ -0.02 \end{bmatrix}$	\mathbf{b}_{f11} $= \begin{bmatrix} -0.32 \\ -0.32 \\ -0.00 \end{bmatrix}$	\mathbf{b}_{sa11} $= \begin{bmatrix} -0.66 \\ -0.27 \\ -0.00 \end{bmatrix}$
2	\mathbf{b}_{o12} $= \begin{bmatrix} 0.63 \\ -0.65 \\ -0.02 \end{bmatrix}$	\mathbf{b}_{f12} $= \begin{bmatrix} 0.32 \\ -0.32 \\ -0.00 \end{bmatrix}$	\mathbf{b}_{sa12} $= \begin{bmatrix} -0.57 \\ -0.47 \\ -0.00 \end{bmatrix}$

Table 2 (continue)

j	s_{pijx}	s_{pijy}	s_{pijz}
1	\mathbf{b}_{sp11x} $= \begin{bmatrix} -0.71 \\ 0.71 \\ 0.01 \end{bmatrix}$	\mathbf{b}_{sp11y} $= \begin{bmatrix} 0.25 \\ 0.25 \\ 0.00 \end{bmatrix}$	\mathbf{b}_{sp11z} $= \begin{bmatrix} -0.06 \\ -0.06 \\ -0.00 \end{bmatrix}$
2	\mathbf{b}_{sp12x} $= \begin{bmatrix} -0.71 \\ -0.71 \\ -0.01 \end{bmatrix}$	\mathbf{b}_{sp12y} $= \begin{bmatrix} -0.24 \\ 0.26 \\ 0.00 \end{bmatrix}$	\mathbf{b}_{sp12z} $= \begin{bmatrix} 0.06 \\ -0.06 \\ 0.00 \end{bmatrix}$

7. Conclusions

In order to obtain appropriate grasps, we treated grasp stability from the viewpoint of potential energy. Frictionless enveloping grasps in two dimensions was investigated. Not only joint position displacements but also link surface displacements are replaced with elastic properties. The potential energy of the grasp system including the displacements was derived. The wrench vector and the grasp stiffness matrix were obtained by the first and the second partial derivatives, respectively. The derivatives are formulated in an analytical way. It is shown that the wrench and the matrix are given by functions of the grasp parameters. Using partial derivatives of the stiffness matrix by local curvatures at contact points, the local curvature effects on the grasp stability were clarified. Stiffness effects were also derived. To confirm validity of our analysis, we showed a numerical example.

Using our analysis, a grasp system can be evaluated when contact positions, contact directions, local curvatures, spring stiffnesses, and so on are inputted. Consequently, this method can be used for searching an optimum grasp and/or generating training data for machine learning.

In [9], we considered masses of the object and finger links in the analysis. We can also include the masses in this paper but omitted due to page space.

The case of rolling contact at contact points was omitted due to page space. We will discuss the case in our future publication. In our future work, we will discuss three dimensional grasps.

References

- [1] M. S. Siddiqui, C. Coppola, G. Solak L. Jamone, Grasp Stability Prediction for a Dexterous Robotic Hand Combining Depth Vision and Haptic Bayesian Exploration, *Frontiers in Robotics and AI*, Vol. 8, Article 703869, 2021.
- [2] T. Li, X. Sun, X. Shu, C. Wang, Y. Wang, G. Chen, N. Xue, Robot Grasping System and Grasp Stability Prediction Based on Flexible Tactile Sensor Array, *MDPI Machines*, Vol. 9, No. 6, p. 119, 2021.
- [3] H. Dang, P. K. Allen, Learning Grasp Stability, *Proc. IEEE ICRA2012*, p. 2392-2397, 2012.
- [4] H. Hanafusa, H. Asada, Stable Prehension of Objects by the Robot Hand with Elastic Fingers, *J. SICE*, Vol. 13, No. 4, p. 370, 1977.

[5] V. D. Nguyen, Constructing Stable Grasps, Int. J. Robotics Research, Vol. 8, No. 1, pp. 26-37, 1989.

[6] T. Watanabe, Softness effects on manipulability and grasp stability, Proc. IEEE/RSJ IROS2011, 2011.

[7] H. Dong, C. Qiu, D. K. Prasad, Y. Pan, J. Dai, I-M. Chen, Enabling grasp action: Generalized quality evaluation of grasp stability via contact stiffness from contact mechanics insight, Elsevier Mechanism and Machine Theory, No. 134, p.625-644, 2019.

[8] T. Yamada, T. Taki, M. Yamada, H. Yamamoto, Static Grasp Stability Analysis of Two Spatial Objects Including Contact Surface Geometry, Transaction on Control and Mechanical Systems, Vol. 1, No. 5, p. 218-228, 2012.

[9] T. Yamada, R. Johansson, A. Robertsson, H. Yamamoto, Static Stability Analysis of a Planar Object Grasped by Multifingers with Three Joints, Robotics, Vol. 4, No. 4, pp. 464-491.

[10] T. Yamada, K. Niwa, H. Yamamoto, H. Kawasaki, T. Mouri, Automatic generation of grasp positions using the partial differentiation of the grasp stiffness matrix, J. of Robotic and Mechatronic Systems, Vol. 2, No. 2, pp. 1-15, 2017.

Appendix A: Vectors and matrices

In planar case, a homogeneous transformation matrix of frame Σ_b with respect to frame Σ_a is denoted as

$${}^aA_b := \begin{bmatrix} {}^aR_b & {}^a\mathbf{p}_b \\ 0_{1 \times 2} & 1 \end{bmatrix} \in \mathbb{R}^{3 \times 3} \quad (42)$$

where ${}^a\mathbf{p}_b \in \mathbb{R}^2$ is a position vector and ${}^aR_b \in \mathbb{R}^{2 \times 2}$ is a rotation matrix. We use the following vectors and matrices:

$$\begin{aligned} \mathbf{u}_1 &:= \begin{bmatrix} 1 \\ 0 \end{bmatrix}, \quad \mathbf{u}_2 := \begin{bmatrix} 0 \\ 1 \end{bmatrix}, \quad \mathbf{z} := \begin{bmatrix} 1 \\ -1 \end{bmatrix} \\ \mathbf{v}_x &:= \begin{bmatrix} \mathbf{u}_1 \\ 0 \end{bmatrix}, \quad \mathbf{v}_y := \begin{bmatrix} \mathbf{u}_2 \\ 0 \end{bmatrix}, \quad \mathbf{v}_\zeta := \begin{bmatrix} 0_{2 \times 1} \\ 1 \end{bmatrix} \\ \boldsymbol{\varepsilon} &:= \begin{bmatrix} x \\ \zeta \end{bmatrix}, \quad \mathbf{x} := \begin{bmatrix} x \\ y \end{bmatrix} \\ \text{Rot}(\zeta) &:= \begin{bmatrix} \cos \zeta & -\sin \zeta \\ \sin \zeta & \cos \zeta \end{bmatrix}, \\ \Omega &:= \begin{bmatrix} 0 & -1 \\ 1 & 0 \end{bmatrix} = \text{Rot}\left(\frac{\pi}{2}\right) \\ A_t(\mathbf{x}) &:= \begin{bmatrix} I_2 & \mathbf{x} \\ 0_{1 \times 2} & 1 \end{bmatrix}, \quad A_r(\zeta) := \begin{bmatrix} \text{Rot}(\zeta) & 0_{2 \times 1} \\ 0_{1 \times 2} & 1 \end{bmatrix} \\ A_{tr}(\boldsymbol{\varepsilon}) &:= A_t(\mathbf{x})A_r(\zeta), \\ {}^aB_b &:= \begin{bmatrix} {}^aR_b & -\Omega {}^a\mathbf{p}_b \\ 0_{1 \times 2} & 1 \end{bmatrix}, \quad I_{23} = [I_2 \quad 0_{2 \times 1}] \in \mathbb{R}^{2 \times 3} \\ {}^aW_b &:= \begin{bmatrix} {}^aR_b \\ {}^a\mathbf{p}_b \times {}^aR_b \end{bmatrix} = [I_{23} \quad {}^bB_a]^T \end{aligned} \quad (43)$$

Appendix B: Partial derivatives of U_{iq}

The second partial derivatives of U_{iq} are obtained as follows:

$$\begin{aligned} U_{iq, \varepsilon \alpha_k} &:= \left. \frac{\partial^2 U_{iq}(\boldsymbol{\varepsilon}_o, \boldsymbol{\alpha}_i, \boldsymbol{\beta}_i)}{\partial \boldsymbol{\varepsilon}_o \partial \boldsymbol{\alpha}_{ik}^T} \right|_0 \\ &= {}^{Lfik} B_o^T S_{pik} K_{ik} + \mathbf{v}_\zeta (\mathbf{v}_x^T \boldsymbol{\tau}_{pik}) \begin{bmatrix} 1 \\ 1 \end{bmatrix}^T \\ U_{iq, \varepsilon q_k} &:= \left. \frac{\partial^2 U_{iq}(\boldsymbol{\varepsilon}_o, \boldsymbol{\alpha}_i, \boldsymbol{\beta}_i)}{\partial \boldsymbol{\varepsilon}_o \partial q_{daik}} \right|_0 \\ &= - \sum_{j=k}^n {}^{Lfij} B_o^T [S_{pij} {}^{Lfij} B_{ik} \mathbf{v}_\zeta + I_{23}^T \Omega I_{23} \boldsymbol{\tau}_{pij}] \\ U_{iq, \alpha_l \alpha_k} &:= \left. \frac{\partial^2 U_{iq}(\boldsymbol{\varepsilon}_o, \boldsymbol{\alpha}_i, \boldsymbol{\beta}_i)}{\partial \boldsymbol{\alpha}_{il} \partial \boldsymbol{\alpha}_{ik}^T} \right|_0 \\ &= \begin{cases} K_{il}^T S_{pik} K_{ik} + (\mathbf{v}_x^T \boldsymbol{\tau}_{pik}) \begin{bmatrix} \kappa_{oik} & \kappa_{oik} \\ \kappa_{oik} & -\kappa_{fik} \end{bmatrix} & (l = k) \\ 0_{2 \times 2} & (\text{otherwise}) \end{cases} \\ U_{iq, q_l \alpha_k} &:= \left. \frac{\partial^2 U_{iq}(\boldsymbol{\varepsilon}_o, \boldsymbol{\alpha}_i, \boldsymbol{\beta}_i)}{\partial q_{dail} \partial \boldsymbol{\alpha}_{ik}^T} \right|_0 \\ &= \begin{cases} -\mathbf{v}_\zeta^T {}^{Lfik} B_{il}^T S_{pik} K_{ik} - (\mathbf{v}_x^T \boldsymbol{\tau}_{pik}) [1 \quad 1] & (l \leq k) \\ 0_{1 \times 2} & (\text{otherwise}) \end{cases} \\ U_{iq, q_l q_k} &:= \left. \frac{\partial^2 U_{iq}(\boldsymbol{\varepsilon}_o, \boldsymbol{\alpha}_i, \boldsymbol{\beta}_i)}{\partial q_{dail} \partial q_{daik}} \right|_0 \\ &= \begin{cases} S_{aik} + \sum_{j=k}^n [\mathbf{v}_\zeta^T {}^{Lfij} B_{il}^T S_{pij} {}^{Lfij} B_{ik} \mathbf{v}_\zeta + \boldsymbol{\tau}_{pij}^T I_{23}^T {}^{Lfij} \mathbf{p}_{ik}] & (l = k) \\ \sum_{j=k}^n [\mathbf{v}_\zeta^T {}^{Lfij} B_{il}^T S_{pij} {}^{Lfij} B_{ik} \mathbf{v}_\zeta + \boldsymbol{\tau}_{pij}^T I_{23}^T {}^{Lfij} \mathbf{p}_{ik}] & (k \leq l \leq j) \end{cases} \end{aligned} \quad (44)$$

$$\begin{aligned} &\frac{\partial}{\partial \boldsymbol{\varepsilon}_o} \left[\frac{\partial U_{iq}(\boldsymbol{\varepsilon}_o, \boldsymbol{\alpha}_i, \boldsymbol{\beta}_i)}{\partial \boldsymbol{\alpha}_i^T} \quad \frac{\partial U_{iq}(\boldsymbol{\varepsilon}_o, \boldsymbol{\alpha}_i, \boldsymbol{\beta}_i)}{\partial \boldsymbol{\beta}_i^T} \right] \\ &= \left[\frac{\partial^2 U_{iq}(\boldsymbol{\varepsilon}_o, \boldsymbol{\alpha}_i, \boldsymbol{\beta}_i)}{\partial \boldsymbol{\varepsilon}_o \partial \boldsymbol{\alpha}_i^T} \quad \frac{\partial^2 U_{iq}(\boldsymbol{\varepsilon}_o, \boldsymbol{\alpha}_i, \boldsymbol{\beta}_i)}{\partial \boldsymbol{\varepsilon}_o \partial \boldsymbol{\beta}_i^T} \right] \\ &+ \left[\frac{\partial \boldsymbol{\alpha}_i^T}{\partial \boldsymbol{\varepsilon}_o} \quad \frac{\partial \boldsymbol{\beta}_i^T}{\partial \boldsymbol{\varepsilon}_o} \right] \begin{bmatrix} \frac{\partial^2 U_{iq}(\boldsymbol{\varepsilon}_o, \boldsymbol{\alpha}_i, \boldsymbol{\beta}_i)}{\partial \boldsymbol{\alpha}_i \partial \boldsymbol{\alpha}_i^T} & \frac{\partial^2 U_{iq}(\boldsymbol{\varepsilon}_o, \boldsymbol{\alpha}_i, \boldsymbol{\beta}_i)}{\partial \boldsymbol{\alpha}_i \partial \boldsymbol{\beta}_i^T} \\ \frac{\partial^2 U_{iq}(\boldsymbol{\varepsilon}_o, \boldsymbol{\alpha}_i, \boldsymbol{\beta}_i)}{\partial \boldsymbol{\beta}_i \partial \boldsymbol{\alpha}_i^T} & \frac{\partial^2 U_{iq}(\boldsymbol{\varepsilon}_o, \boldsymbol{\alpha}_i, \boldsymbol{\beta}_i)}{\partial \boldsymbol{\beta}_i \partial \boldsymbol{\beta}_i^T} \end{bmatrix} \\ &= [0_{3 \times 2n} \quad 0_{3 \times n}] \end{aligned} \quad (45)$$

Appendix C: Curvature effects

The second partial derivatives of U_{iq} are obtained as follows:

$$\begin{aligned}
\frac{\partial U_{iq,\varepsilon\varepsilon}}{\partial \kappa_{oik}} &= \mathbf{0}_{3 \times 3}, \quad \frac{\partial U_{iq,\beta\beta}}{\partial \kappa_{oik}} = \mathbf{0}_{n \times n}, \\
\frac{\partial U_{iq,\varepsilon\beta}}{\partial \kappa_{oik}} &= \frac{\partial U_{iq,\beta\varepsilon}^T}{\partial \kappa_{oik}} = \mathbf{0}_{3 \times n}, \\
\frac{\partial U_{iq,\alpha\varepsilon}^T}{\partial \kappa_{oik}} &= \frac{\partial U_{iq,\varepsilon\alpha}}{\partial \kappa_{oik}} = \frac{U_{iq,\varepsilon\alpha} \mathbf{z}}{\kappa_{oik} + \kappa_{fik}} \begin{bmatrix} \mathbf{0}_{2(k-1) \times 1} \\ \mathbf{u}_1 \\ \mathbf{0}_{2(n-k) \times 1} \end{bmatrix}^T \in \mathbb{R}^{3 \times 2n}, \\
\frac{\partial U_{iq,\alpha\alpha}}{\partial \kappa_{oik}} &= \begin{bmatrix} \mathbf{0}_{2(k-1) \times 1} \\ \mathbf{u}_1 \\ \mathbf{0}_{2(n-k) \times 1} \end{bmatrix} \begin{bmatrix} \mathbf{0}_{2(k-1) \times 1} \\ \frac{U_{iq,\alpha\alpha} \mathbf{z}}{\kappa_{oik} + \kappa_{fik}} \\ \mathbf{0}_{2(n-k) \times 1} \end{bmatrix}^T \\
&+ \begin{bmatrix} \mathbf{0}_{2(k-1) \times 1} \\ \frac{U_{iq,\alpha\alpha} \mathbf{z}}{\kappa_{oik} + \kappa_{fik}} \\ \mathbf{0}_{2(n-k) \times 1} \end{bmatrix} \begin{bmatrix} \mathbf{0}_{2(k-1) \times 1} \\ \mathbf{u}_1 \\ \mathbf{0}_{2(n-k) \times 1} \end{bmatrix}^T \\
&+ [{}^L f_{ik} \mathbf{f}^T \mathbf{u}_1] \begin{bmatrix} \mathbf{0}_{2(k-1) \times 1} \\ \mathbf{u}_1 \\ \mathbf{0}_{2(n-k) \times 1} \end{bmatrix} \begin{bmatrix} \mathbf{0}_{2(k-1) \times 1} \\ \mathbf{u}_1 \\ \mathbf{0}_{2(n-k) \times 1} \end{bmatrix}^T, \\
\frac{\partial U_{iq,\alpha\beta}^T}{\partial \kappa_{oik}} &= \frac{\partial U_{iq,\beta\alpha}}{\partial \kappa_{oik}} \\
&= \begin{bmatrix} \mathbf{0}_{n \times 2(k-1)} & \frac{U_{iq,\beta\alpha} \mathbf{z}}{\kappa_{oik} + \kappa_{fik}} \mathbf{u}_1^T & \mathbf{0}_{n \times 2(n-k)} \end{bmatrix}.
\end{aligned} \tag{44}$$

Authors Introduction

Dr. Takayoshi Yamada



He is a Professor with the Department of Mechanical Engineering, Gifu University. He received the B.E., M.E, Ph.D. degrees in Mechanical Engineering from the Nagoya Institute of Technology, Japan, in 1991, 1993, 1995, respectively. He is a member of the Japan Society of Mechanical Engineers (JSME), the Robotics Society of Japan (RSJ), the Society of Instrument and Control Engineers (SICE), IEEE, and the Japan Society of Precision Engineering (JSPE). His research interests include grasping, manipulation, sensing, and automation systems.

Dr. Hidehiko Yamamoto



He is currently a specially appointed professor, Gifu University. He received the M.E. and Ph. D. degrees in Mech. Eng. from Nagoya Institute of Technology, in 1980, 1991. He was a professor with the Department. of Mechanical Engineering, Gifu University.
